Inorg. Chem. **2008**, *47*, 4520−4530

Iron Tetraanthracenotetraazaporphyrins: Synthesis, Structural Characterization, Ligand Binding Properties, and Unexpected Selectivity of a Bis-"Bowl" Tetraazaporphyrin

Jeffrey P. Fitzgerald,* Joshua R. Lebenson, Guangbin Wang, Gordon T. Yee, Bruce C. Noll, and Roger D. Sommer

Departments of Chemistry, United States Naval Academy, Annapolis, Maryland 21402, Virginia Polytechnic Institute and State University, Blacksburg, Virginia 24061, DePaul University, Chicago, Illinois 60614, and Department of Chemistry and Biochemistry, University of Notre Dame, Notre Dame, Indiana 46556

Received November 1, 2007

The synthesis and characterization, by optical spectroscopy, mass spectrometry, superconducting quantum interference device (SQUID) magnetometry, and single-crystal X-ray diffraction, of six iron complexes of tetraanthracenotetraazaporphyrin (TATAP) are reported. Eight benzo groups, flanking the macrocycle periphery, form a nonpolar "bowl" on each face of the porphyrazine and prevent μ-oxo dimer formation. Fe(TATAP) readily binds THF, a variety of neutral nitrogenous axial ligands, and carbon monoxide. The equilibrium binding constants for the first two are higher than those of analogous porphyrins while those of the latter are smaller. We attribute these differences to the higher π acidity of the porphyrazine ligand. Fe(TATAP) also shows different relative magnitudes of the successive equilibrium binding constants, K_1 and K_2, for hindered nitrogenous ligands when compared to those of porphyrin analogues. Surprisingly, Fe(TATAP), in toluene solution, shows no affinity for O_2 when exposed to 1 atm partial pressure of O_2 at 25 °C. These results are explained in terms of an unusually positive iron(III/II) redox potential when coordinated by the TATAP ligand.

Introduction

The reversible binding of oxygen and carbon monoxide by ferrous porphyrins and the factors affecting the kinetics and thermodynamics of these processes have been extensively studied since Perutz's[1] and Kendrew's[2] Nobel prize-winning structural characterization of hemoglobin. Over the intervening decades, successive generations of porphyrin-based biomimetic models have explored the effects of solvent polarity, axial ligand basicity, axial ligand strain, distal-side steric hindrance, distal-side polarity, and distal-side hydrogen bonding on the differential binding of dioxygen and carbon monoxide.[3]

Discrimination between the gaseous ligands dioxygen and carbon monoxide in these complexes is given by *M*, defined as the ratio $P_{1/2}(O_2)/P_{1/2}(CO)$, where $P_{1/2}(O_2)$ and $P_{1/2}(CO)$ are the half-saturation pressures for oxygen and carbon monoxide, respectively. Large values of *M* indicate a preference for CO binding over O_2. *M* values for biological heme-based oxygen carriers range from 20 (myoglobin) to 150 (T-state hemoglobin) while *M* values for synthetic analogues range from <0.003 to 180000. In general, complexes with nonpolar, unobstructed ligand binding cavities and appended axial ligands exhibit the largest *M* values.[3c]

We report herein the synthesis, characterization, and ligand binding properties of iron complexes of tetraanthracenotetraazaporphyrin (TATAP).[4] In this ligand, four anthracene units, bonded by their central ring to the β-pyrrolic carbons of the porphyrazine macrocycle, form an open and nonpolar ligand binding cavity on each face of the macrocycle. In spite

* To whom correspondence should be addressed. E-mail: fitzgera@usna.edu. Fax: 410-293-2218.

(1) (a) Perutz, M. *Nature* **1970**, *228*, 726–734. (b) Perutz, M. F. *Br. Med. Bull.* **1976**, *32*, 193–208. (c) Perutz, M. F. *Sci. Am.* **1978**, *239*, 92–125. (d) Perutz, M. F. *Annu. Rev. Biochem.* **1979**, *48*, 327–386.

(2) Nobbs, C. L.; Watson, H. C.; Kendrew, J. C. *Nature* **1966**, *209*, 339–341.

(3) (a) Momenteau, M.; Reed, C. A. *Chem. Rev.* **1994**, *94*, 659–698. (b) Collman, J. P.; Fu, L. *Acc. Chem. Res.* **1999**, *32*, 455–463. (c) Collman, J. P.; Boulatov, R.; Sunderland, C. J.; Fu, L. *Chem. Rev* **2004**, *104*, 561–588, and references therein.

(4) This ligand is also known as dibenzobarrelenoporphyrazine.

10.1021/ic702149z CCC: $40.75 © 2008 American Chemical Society
Published on Web 05/07/2008

Scheme 1

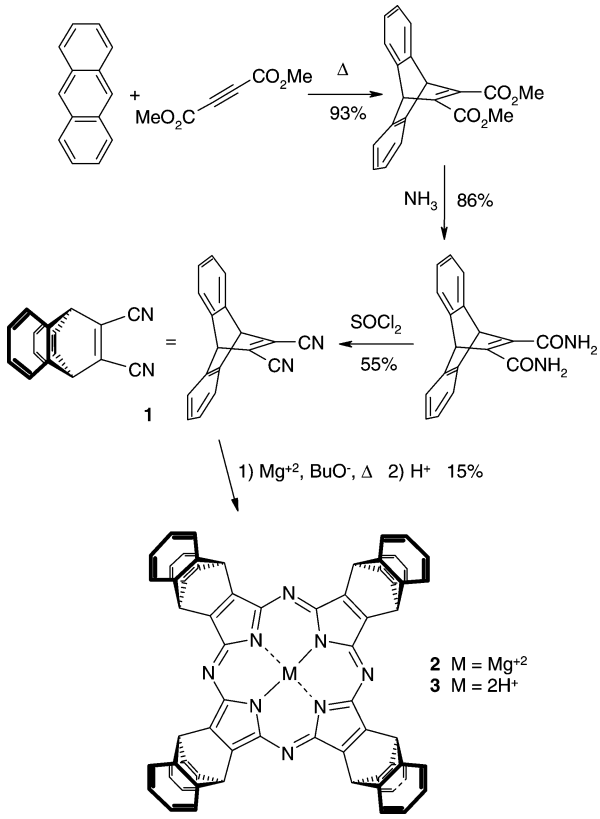

of being known for over 30 years,[5] the coordination chemistry of this interesting ligand is essentially unexplored. We find that the four-coordinate iron(II) derivative, Fe(TATAP), reversibly binds a variety of neutral ligands such as THF, nitrogenous bases, and carbon monoxide, and we report here equilibrium binding constants. Surprisingly, Fe(TATAP) at room temperature shows no affinity for dioxygen, giving an undefined *M* value. This behavior is in stark contrast to that of all previously reported iron(II) porphyrins and tetraazaporphyrins, which either bind O_2 reversibly or react irreversibly to give a μ-oxo dimer. The undefined selectivity of Fe(TATAP) for CO over O_2 may be the result of a positively shifted iron(III/II) redox potential, a heretofore unrecognized factor in CO/O_2 discrimination in biomimetic complexes. Our results suggest a possible application as a carbon monoxide detector.

Results and Discussion

Ligand Synthesis. Kopranenkov prepared magnesium tetraanthracenotetraazaporphyrin, **2**, Mg(TATAP), by the cyclocondensation of dinitrile, **1**, the product of a Diels–Alder reaction between anthracene and dicyanoacetylene, under Linstead conditions.[5] Our inability to scale up the synthesis of dicyanoacetylene led us to make minor modifications to the procedure of Smith, as shown in Scheme 1, to make

(5) (a) Kopranenkov, V. N.; Rumyantseva, G. I.; Luk'yanets, E. A. *Zh. Obshch. Khim.* **1972**, *42*, 2586. (b) Kopranenkov, V. N.; Rumyantseva, G. I. *J. Gen. Chem.* **1975**, *45*, 1521–1524.

(6) Oliver, S. W.; Smith, T. D. *J. Chem Soc., Perkin Trans. 2* **1987**, 1579–1582.

Scheme 2

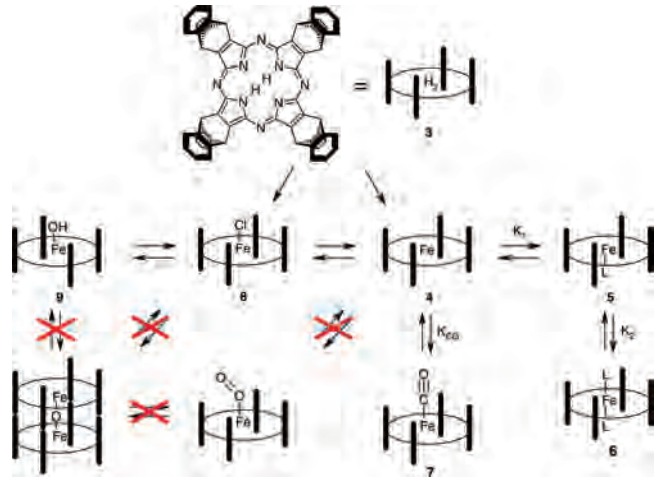

Mg(TATAP), **2**.[6] The crude product is typically not isolated but instead heated at reflux in a chloroform solution containing a small amount of acetic acid to give gram quantities of the unmetalated analogue, H_2(TATAP), **3**, in reproducible, albeit low, yields of 12−18%. This material, which has a visible spectrum identical to that reported by Kopranenkov, has been further characterized by elemental analysis, X-ray crystallography,[7] IR spectroscopy, ^{1}H NMR spectroscopy, and matrix-assisted laser desorption ionization time-of-flight (MALDI-TOF) mass spectrometry. Our combined yield for the cyclization and demetalation steps is lower than that reported by Kopranenkov et al.,[5] who characterized the product only by elemental analysis and visible spectroscopy. However, since little difference is expected between the elemental analyses of the dinitrile precursor and the macrocyclic product, the yield reported by Kopranenkov may not be accurate.

Iron Complex Synthesis and Coordination Chemistry. The synthesis and coordination chemistry of iron complexes of TATAP are summarized in Scheme 2. The insertion of iron into H_2(TATAP) was accomplished by the same procedure used for metalating the unhindered octaethyltetraazaprophyrin, H_2(OETAP), adjusting for the lower solubility of the anthraceno-appended macrocycle.[8] Like related iron(II) macrocycles, **4** readily binds one or two axial ligands to form five-coordinate, **5**, or six-coordinate, **6**, complexes, respectively. Fe(TATAP) will also bind 1 equiv of gaseous carbon monoxide to form the carbonyl adduct, **7**. Surprisingly, **4** shows no measurable affinity for gaseous oxygen even at a partial pressure of 1 atm, nor do we see any evidence for μ-oxo dimer formation. The iron(II) complex **4** can be oxidized to the five-coordinate chloroiron(III) tetraanthracenotetraazaporphyrin, Fe(TATAP)Cl, **8**. As expected for a complex bearing large peripheral groups, treatment of **8** with aqueous base yields the hydroxo adduct, **9**, not the μ-oxo dimer. The treatment of **9** with aqueous HCl will re-form **8**. Both of the iron(III) complexes, **8** and **9**, can be reduced to **4**.

(7) Rheingold, A. L. University of California, San Diego, CA, personal communication.

(8) Fitzgerald, J. P.; Haggerty, B. S.; Rheingold, A. L.; May, L.; Brewer, G. A. *Inorg. Chem.* **1992**, *31*, 2006–2013.

Table 1. UV–Visible Spectroscopic Information for Complexes **2–9**

		absorption maxima (nm) (log ε)						
no.	cmpd	B band			Q band			
2	Mg(TATAP)	371 (4.80)			547 (4.07)	595 (4.92)		
3	H_2(TATAP)	346 (4.82)	412 (4.39)			558 (4.68)		
						634 (4.85)		
4	Fe(TATAP)	<300	418 (sh)	496 (4.42)	554 (4.56)	588 (4.60)	646 (4.25)	
5	Fe(TATAP)(quin)	<300	414 (sh)	520 (4.65)		572 (4.59)	646 (4.13)	746 (4.05)
6	Fe(TATAP)(pyr)$_2$	356 (4.88)	496 (4.35)	548 (4.50)	570 (4.63)	590 (4.98)		
7	Fe(TATAP)CO	368 (4.69)	430 (sh)	530 (sh)		572 (4.93)	654 (3.82)	
8	Fe(TATAP)Cl	324 (4.66)	432 (4.48)	516 (4.46)		640 (sh)	672 (4.22)	
9	Fe(TATAP)OH	324 (4.63)	432 (4.45)	506 (4.20)		618 (4.65)	672 (3.86)	

UV−Visible Spectra. The various complexes in Scheme 2 exhibit unique UV–visible spectra that are compiled in Table 1. These spectra may be qualitatively interpreted using Gouterman's four-orbital model.[9]

The visible spectrum of Mg(TATAP), dominated by strong absorbance at 371 and 595 nm (the B and Q bands, respectively), is characteristic of porphyrazines bonded to closed-shell M^{2+} ions. The Q band splits into two peaks when **2** is converted to **3**, consistent with a reduction in the molecular symmetry from D_{4h} to D_{2h}. The optical spectroscopy of **2** and **3** is nearly identical to that of the analogous octaethyltetraazaporphyrin (OETAP) complexes,[10] indicating that the bridged anthracene appendages in TATAP do not significantly alter the relative energies of Gouterman's four π orbitals.

Metalation with iron(II) restores the 4-fold symmetry and a single Q band with additional absorbance maxima appearing due to charge-transfer (CT) transitions. Surprisingly, the B bands in both **4** and **5** are blue-shifted below 300 nm, likely due to mixing with a nearby CT band. Formation of the six-coordinate complexes tends to sharpen the Q band (with a concomitant increase in molar absorptivity) and restores the B band to its normal range. Comparison to the optical spectra of analogous iron(II) OETAP complexes reveals nearly identical λ_{max} values for the Q bands but blue-shifted B bands.[8] Finally, the iron(III) complexes, **8** and **9**, show a blue shift in the B band but a red shift in the Q band when compared to those of the iron(II) analogues. These shifts are similar to those observed when comparing the spectra of iron(II) versus iron(III) OETAP complexes.

Iron(III) Complexes. Chloroiron(III) tetraanthracenotetraazaporphyrin, **8**, can be prepared directly from the free-base macrocycle by heating in DMF in the presence of an iron salt followed by an aqueous workup.[11] Alternatively, **8** can be made by oxidation of the square-planar four-coordinate iron(II) complex. Fe(TATAP)Cl, **8**, has been characterized by elemental analysis, UV–visible spectroscopy, and IR spectroscopy. MALDI-TOF mass spectrometry shows a weak molecular ion peak at 1109 amu and a strong base peak at 1073 amu, consistent with the loss of a chloride ion. Superconducting quantum interference device (SQUID) magnetic susceptibility measurements, shown in Figure 1, reveal linear Curie–Weiss behavior over the temperature range 5−300 K with a magnetic moment varying between 4.34 and 4.52 μ_B with $C = 2.47$ emu K/mol and $\theta \sim 0$. This data is consistent with an intermediate-spin $S = {}^3/_2$ d^5 system, like that observed for related iron(III) porphyrazines,[8,12] and is supported by X-ray crystallographic studies.

Unlike the cases of planar porphyrins[13] and azaporphyrins,[8] shaking an organic solution of **8** with an aqueous base does not result in the formation of the μ-oxo dimer. Instead, an emerald-green complex is formed, which has been characterized by elemental analysis, UV–visible and IR spectroscopy, MALDI-TOF mass spectrometry, and magnetic susceptibility measurements, as intermediate-spin hydroxyiron(III) tetraanthracenotetraazaporphyrin, Fe(TATAP)OH, **9**. Analysis of the magnetic susceptibility data for **9** was complicated by a temperature-independent contribution, which we attribute to a trace ferromagnetic impurity. Correcting for this impurity gave an excellent fit of the experimental data to the Curie–Weiss law. Even with the impurity, a room-temperature moment of 5.4 μ_B was observed. This is smaller than the 5.8 μ_B moment observed for Fe(TMP)OH,[14] a high-spin iron(III) porphyrin complex, and smaller than the expected $S = {}^5/_2$ spin-only moment of 5.92 μ_B. Subtracting the temperature-independent component, determined by a fit to the Curie Law, from the experimental susceptibility yields a room-temperature moment of 4.4 μ_B for **9**, consistent with the intermediate-spin $S = {}^3/_2$ assignment. There is no evidence in either the magnetic susceptibility measurements or the ^{1}H NMR spectrum for the diamagnetic μ-oxo dimer. Formation of **9** is reversible; shaking a solution of **9** with aqueous HCl rapidly yields **8**.

The inability of iron tetraanthracenotetraazaporphyrin to form a μ-oxo dimer, either by reaction of the chloroiron(III) derivative with an aqueous base or by air oxidation of the iron(II) derivative (vide infra), was expected. The four benzo groups flanking each face of the tetraazaporphyrin macrocycle prevent two iron atoms from approaching close enough to be bound

(9) Gouterman, M. In *The Porphyrins, Vol. III, Part A Physical Chemistry*; Dolphin, D., Ed.; Academic Press: New York, 1978; pp 1–165.
(10) Fitzgerald, J.; Taylor, W.; Owens, H. *Synthesis* **1991**, 686–688.
(11) (a) Adler, A. D.; Longo, F. R.; Kampas, F.; Kim, J. *J. Inorg. Nucl. Chem.* **1970**, *32*, 2443. (b) Walker, J. A.; LaMar, G. N. *Ann. N.Y. Acad. Sci.* **1973**, *206*, 328–348. (c) Buckingham, D. A.; Clark, C. R.; Webley, W. S. *J. Chem. Soc., Chem. Commun.* **1981**, 192–194. (d) Tomoda, H.; Saito, S.; Shiraishi, S. *Chem. Lett.* **1983**, 313–316.
(12) Fitzgerald, J. P.; Yap, G. P. A.; Rheingold, A. L.; Brewer, C. T.; May, L.; Brewer, G. A. *J. Chem. Soc., Dalton Trans.* **1996**, 1249–1253.
(13) (a) Sadasivan, N.; Eberspraecher, H. I.; Fuchsman, W. H.; Caughey, W. S. *Biochemistry* **1969**, *8*, 534–541. (b) Cohen, I. A. *J. Am. Chem. Soc.* **1969**, *91*, 1980–1983. (c) Hoffman, A. B.; Collins, D. M.; Day, V. W.; Fleischer, E. B.; Srivastava, T. S.; Hoard, J. L. *J. Am. Chem. Soc.* **1972**, *94*, 3620–3626.
(14) Cheng, R.-J.; Latos-Grazynski, L.; Balch, A. L. *Inorg. Chem.* **1982**, *21*, 2412–2418.

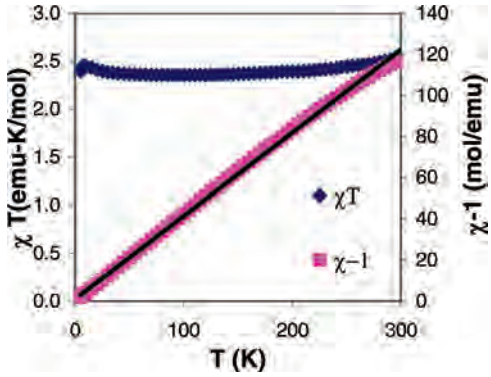

Figure 1. Magnetic susceptibility data for **8**.

Table 2. Crystallographic Data for **8**, Fe(TATAP)Cl

chemical formula	$C_{90}H_{58}Cl_{19}FeN_8$	V (Å^3)	2306.39(4)
formula weight	1980.84	Z	1
space group	$P\bar{1}$ (No. 2)	T (°C)	−150(2)
a (Å)	13.0455(1)	λ (Å)	0.71073
b (Å)	13.8818(1)	D_{obsd} (g cm^{-3})	1.426
c (Å)	14.8536(2)	μ (cm^{-1})	0.763
α (deg)	104.785(1)	R1 (F^2, $I > 2\sigma(I)$)[a]	0.0933
β (deg)	110.180(1)	wR2 (F^2)	0.2587
γ (deg)	102.081(1)	S	1.022

[a] $R1 = \sum||F_o| - |F_c|| / \sum|F_o|$; $wR2 = \sqrt{\sum[w(F_o^2 - F_c^2)^2] / \sum[w(F_o^2)^2]}$; GOF = $S = \sqrt{\sum[w(F_o^2 - F_c^2)^2] / (n-p)}$; n = number of reflections; p = number of parameters refined.

by the same oxygen molecule. This strategy is commonly used to stabilize iron(II) porphyrin complexes.[14,15]

Fe(TATAP)Cl Crystal Structure. The slow evaporation of solvent from a benzene/chloroform solution of **8** caused large cubic crystals to be deposited. The large cavity on each face of the macrocycle resulted in a very open structure that, on refinement, was shown to contain highly disordered solvent molecules. Standard modeling of the solvent was not successful. Accounting for the presence of the solvent and the removal from the refinement process was accomplished with the SQUEEZE routine of PLATON.[16] SQUEEZE determined the solvent accessible volume per unit cell to be 1167 Å^3 and the number of unaccounted electrons to be 426, consistent with two benzenes and six chloroform solvate molecules disordered within the formula unit. These eight solvent molecules contain a total of 432 electrons. Refinements against the reflection file output by SQUEEZE produced a refined structure free of difference map peaks larger than one electron, and the structure converged at an R_1 value of 0.0935. Because of crystallographically imposed symmetry, the iron and chlorine atoms are disordered across the inversion center of this five-coordinate structure. Crystallographic data are given in Table 2 while two different views of the ORTEP diagram, with the atomic numbering scheme, are shown in Figure 2.

Analysis of the extended crystal structure shows that the macrocycles pack efficiently into layers running parallel to the *bc* plane. The separation between layers is 12.38 Å. The

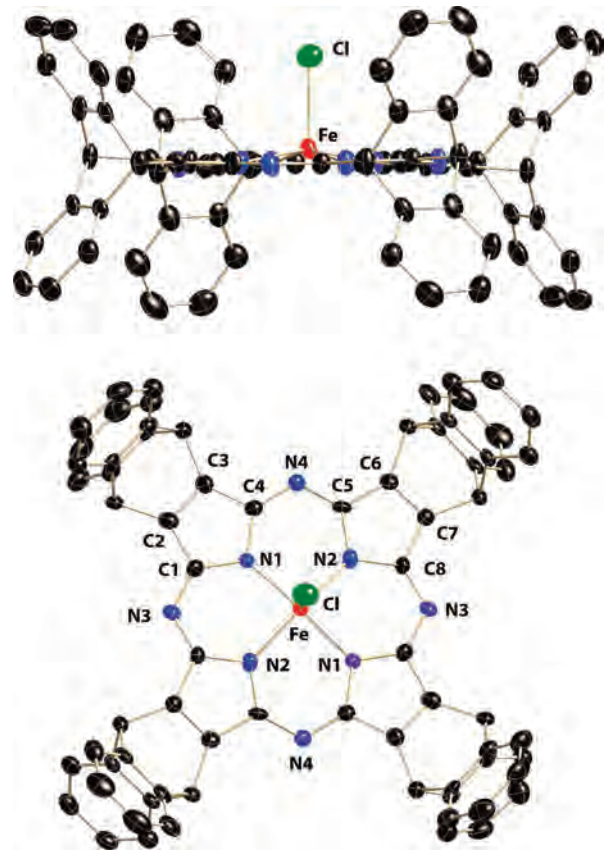

Figure 2. Thermal ellipsoid plot (50% probability) for **8**, Fe(TATAP)Cl. Hydrogen, disordered iron, and chlorine atoms are removed for clarity.

porphyrazine ring is tilted at an angle of 10° relative to the *bc* plane, with the anthraceno group of one macrocycle tucked into the curve of the neighboring macrocycle in an edge-to-face fashion. There is minimal contact between layers, allowing access for the solvents of crystallization. The Fe−Fe distance between layers is 13.05 Å while within a layer the nearest approach of Fe ions is 13.88 Å. The next nearest Fe−Fe distance is 14.85 Å and occurs within a layer.

The porphyrazine macrocycle is essentially planar with an average atom displacement of 0.0894 Å from the mean plane. All eight peripheral benzo rings are planar and are tipped at an average angle of 62° relative to the macrocyle plane, thus forming a bowl-shaped cavity on each face of the macrocycle. The diameter of the bowl varies from 12.5 Å at the base (near the macrocycle) to 14.6 Å at the rim. The depth of the bowl, measured perpendicular to the porphyrazine plane, is 4.2 Å. The four anthraceno groups on the porphyrazine periphery do not prevent small molecule access to the coordinated iron (vide infra) but do provide enough hindrance to prevent direct (via π stacking) or indirect (such as in a μ-oxo dimer) interaction of the iron centers on two different molecules.

The structure of the TATAP ligand is similar to symmetrically superstructured porphyrins such as tetramesitylporphyrin (TMP),[17] tetra(2,4,6-triphenylphenyl)porphyrin (TTPPP),[18] and tetranthracenylporphyrin (TAP),[19] although

(15) (a) Miskelly, G. M.; Webley, W. S.; Clark, C. S.; Buckingham, D. A. *Inorg. Chem.* **1988**, *27*, 3773–3781. (b) Almarsson, O.; Adalsteinsson, H.; Bruice, T. C. *J. Am. Chem. Soc.* **1995**, *117*, 4524–4532.
(16) Spek, A. L. *PLATON: A Multipurpose Crystallographic Tool*; University of Utrecht: Utrecht, The Netherlands, 1997.
(17) Lindsey, J. S.; Wagner, R. W. *J. Org. Chem.* **1989**, *54*, 828–836.
(18) Suslick, K. S.; Fox, M. M. *J. Am. Chem. Soc.* **1983**, *105*, 3507–3510.

access to the metal center may be less constrained. The latter complex differs from TATAP in that the anthracene rings are attached only at the 9 position to the porphyrin *meso* carbons. Except for peripheral groups, porphyrins analogous to TATAP have been reported.[20]

As mentioned above, the iron and chlorine atoms are disordered and occupy either of two equivalent sites on one side or the other of the tetraazaporphyrin ring. The coordination geometry of the iron atom is square pyramidal; the iron atom is displaced from the pyrrolic N plane by 0.3562 Å toward the axial chloride ligand. The iron to chloride bond length is 2.3287(18) Å, and thus, the chloride ligand sits below the rim of the bowl. As demonstrated by Scheidt and Reed,[21] there is a close correlation between the displacement of iron from the macrocycle plane and the occupancy of the $d_{x^2-y^2}$ orbital (i.e., iron spin state) in these complexes. Large displacements (0.46–0.57 Å) are observed in high spin complexes in which an electron in the $d_{x^2-y^2}$ orbital repels the ligand electrons and prevents the iron from dropping into the porphyrin plane. Smaller displacements are observed for low- or intermediate-spin complexes in which this orbital is unoccupied. The observed iron displacement and the average iron to pyrrole nitrogen atom distance of 1.941(3) Å are consistent with an $S = {}^3/_2$ spin state for **8**.

Comparison of the average bond lengths and angles of **8** with those of the "flat" chloroiron(III) complex, Fe(OETAP)-Cl, reveals very few differences except at the macrocycle periphery. The fused bicyclic ring system in the Fe(TATAP) complexes reduces the average $C_\beta-C_\beta-C_{branch}$ bond angle to 115° from 129° in the octaethyl derivative.[8] With this exception, the anthraceno groups fused to the β positions in the TATAP ligand do not distort the macrocycle to any significant extent, consistent with the similarity in UV–visible spectra (vide supra).

Iron(II) Complexes. Heating a toluene/THF solution of **3** in the presence of iron(II) iodide and the hindered base, 2,6-lutidine, gave a nearly quantitative yield of iron(II) tetraanthracenotetraazaporphyrin, Fe(TATAP), **4**. On the basis of elemental analysis, ligand binding studies, and magnetic susceptibility data, and by analogy to related iron(II) porphyrins, **4** is most likely a five-coordinate high-spin ($S = 2$) complex in the solid state. It is possible, however, to interpret the data as an intermediate ($S = 1$) system. In noncoordinating solvents such as toluene, **4** is characterized as a four-coordinate iron(II) complex. Attempts to determine the magnetic susceptibility of **4** in solution by the Evans method were not possible due to its low solubility in noncoordinating solvents.

Elemental analysis and ^{1}H NMR spectroscopy in C_6D_6 with d_5-pyridine clearly indicate the presence of one THF molecule per Fe(TATAP) unit in **4**. In pyridine, **4** is converted to the diamagnetic complex, Fe(TATAP)(pyr)$_2$, **6**. Signals for free THF were observed in the ^{1}H NMR spectrum and quantified by integration. However, it is not clear whether, in the solid state, the THF is coordinated to the iron, giving a five-coordinate complex, or is trapped as a solvate, leaving the iron as four-coordinate. As shown below, Fe(TATAP) will bind one THF ligand ($K_1 = 1400$), which suggests that the THF molecule in **4** is bound. Five-coordinate iron(II) porphyrins are well-known, but these tend to involve porphyrins shielded on one face by "straps" or "pickets",[3] sterically hindered ligands such as 2-substituted imidazoles,[22] or anionic ligands such as the thiolate ion.[23] The two reported complexes between THF and iron(II) porphyrins are both six-coordinate bis-THF adducts;[24] however, both authors note the following: (1) that formation of the bis-THF complex may be driven by its lower solubility and (2) that THF is readily lost from these complexes both in the solid state and in solution.

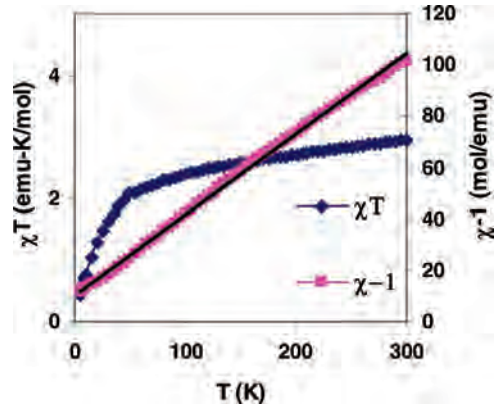

Figure 3. Magnetic susceptibility data for **4.**

A plot of the inverse molar susceptibility for solid **4**, measured as a function of temperature on a SQUID magnetometer, is shown in Figure 3. Linear Curie–Weiss behavior is observed over the entire temperature range examined, 5−300 K, giving a room-temperature effective magnetic moment, $\mu_{eff} = 4.86\ \mu_B$. Analysis of the linear regression yields a Curie constant of 3.19 and a θ value of –32.5.

Possible spin states for a d^6 system are $S = 0$, 1, or 2, for which the spin-only magnetic moments are 0, 2.83, and 4.90 μ_B, respectively. The room-temperature moment of 4.86 μ_B for Fe(TATAP) could be due to either an $S = 1$ complex with a large contribution from unquenched orbital angular momentum or an $S = 2$ spin-only complex. The magnetic susceptibility of Fe(TATAP) is higher than that of planar iron(II) azaporphyrin complexes such as Fe(OETAP)[8] and

(19) Cense, J. M.; Le Quan, R. M. *Tetrahedron Lett.* **1979**, 3725–3728.
(20) (a) Ramondenc, Y.; Schwenninger, R.; Phan, T.; Gruber, K.; Kratky, C.; Krautler, B. *Angew. Chem., Int. Ed. Engl.* **1994**, *33*, 889–891. (b) Schwenninger, R.; Ramondenc, Y.; Wurst, K.; Schlogl, J.; Krautler, B. *Chem.— Eur. J.* **2000**, *6*, 1214–1223.
(21) (a) Scheidt, W. R.; Reed, C. A. *Chem. Rev.* **1981**, *81*, 543–555. (b) Scheidt, W. R. In *The Porphyrin Handbook*; Kadish, K. M., Smith, K. M., Guilard, R., Eds.; Academic Press: San Diego, CA, 2000; Vol. *3*, Chapter 16.
(22) Hoard, J. L. In *Porphyrins and Metalloporphyrins*; Smith, K. M., Ed.; Elsevier: Amsterdam, The Netherlands, 1975; pp 317–380.
(23) Caron, C.; Mitschler, A.; Riviere, G.; Ricard, L.; Schappacher, M.; Weiss, R. *J. Am. Chem. Soc.* **1979**, *101*, 7401–7402.
(24) (a) Kobayashi, H.; Yanagawa, Y. *Bull. Chem. Soc. Jpn.* **1972**, *45*, 450. (b) Collman, J. P.; Gagne, R. R.; Reed, C. A.; Halbert, T. R.; Lang, G.; Robinson, W. T. *J. Am. Chem. Soc.* **1975**, *97*, 1427–1439. (c) Reed, C. A.; Mashiko, T.; Scheidt, W. R.; Spartalian, K.; Lang, G. *J. Am. Chem. Soc.* **1980**, *102*, 2302–2306.

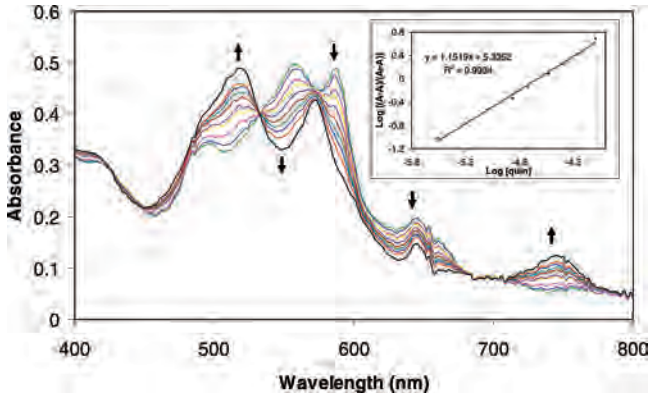

Figure 4. Spectroscopic titration of **4**, Fe(TATAP), with quinuclidine in toluene at 25 °C. $[Fe(TATAP)]_{tot} = 1.1 \times 10^{-5}$ M. [quin] = 0–3.0 × 10^{-3} M.

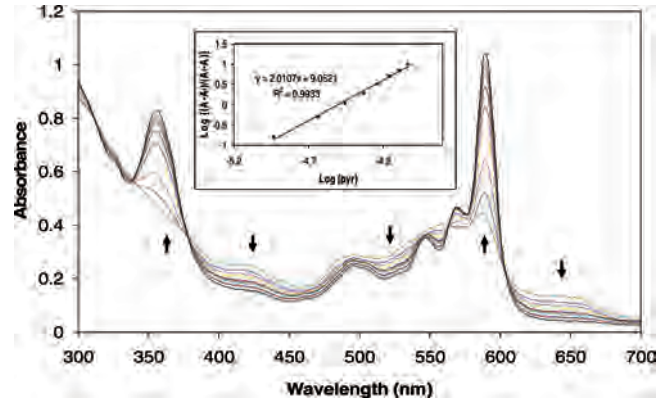

Figure 5. Spectroscopic titration of **4**, Fe(TATAP), with pyridine in toluene at 25 °C. $[Fe(TATAP)]_{tot} = 1.1 \times 10^{-5}$ M. [pyr] = 0–1.0 × 10^{-3} M.

Fe(Pc),[25] which have room-temperature moments of 3.82 and 3.85 μ_B, respectively. The moment of Fe(TATAP) is also higher than that of Fe(TPP),[26] reported as 4.4 μ_B. All three of these related complexes are characterized as four-coordinate, intermediate-spin, $S = 1$ compounds. The measured magnetic moment of **4** is closer to those reported for the high-spin complexes Fe(TPP)(2-MeIm),[27] Fe(TpivPP)(1-MeIm),[28] Fe(TpivPP)$(THF)_2$,[28] Fe(TPP)$(C_2H_5S^-)$,[23] and Fe(TPP)$(THF)_2$,[24] which range from 4.8 to 5.2 μ_B. Given the THF binding study below, the close match between the room-temperature moment of Fe(TATAP) and the expected spin-only moment, and the comparison to related compounds, Fe(TATAP) is most likely a five-coordinate, $S = 2$ complex in the solid state.

Axial Ligand Binding. As shown in Scheme 2, **4** may bind 1 or 2 equivs of axial ligand to give the five- or six-coordinate complexes, respectively. Titrations of toluene solutions of **4** with a variety of neutral axial ligands under anaerobic conditions at 25 °C show isosbestic changes in the visible spectrum, as shown in Figures 4 and 5, consistent with simple two-component equilibria. Analysis of the spectral changes as a function of ligand concentration by the method of Jaffe and Orchin[29] (see Figure insets) allows determination of the number of coordinated ligands (from the slope) and the equilibrium binding constants (from the *y*-intercept). These data are summarized in Table 3.

Addition of either THF or quinuclidine to toluene solutions of **4** results in the decay of absorbances at 554 and 588 nm and the growth in bands at 520, 572, and 746 nm, as shown in Figure 4. Analysis of the absorbance changes indicates coordination of a single axial ligand to form the five-coordinate complex, **5**. For these ligands, $K_1 >> K_2$, and no evidence is seen for the formation of the six-coordinate adduct, **6**. As expected, a larger K_1 value is observed for the more basic quinuclidine ligand. Brault and Rougee have examined THF binding to ferrous porphyrins and observed only the formation of the five-coordinate adduct with K values ~ 5.[30] Thus, THF binds to Fe(TATAP) several orders of magnitude more tightly than it does to iron(II) porphyrins. Larger binding constants to ferrous porphyrazines have been observed with nitrogenous ligands and are attributed to the higher effective charge on iron due to stronger iron-to-macrocycle backbonding in the porphyrazine complexes.[8]

Table 3. Axial Ligation and Equilibrium Binding Constants to **4** at 25 °C

Ligand	Number Bound	K_1	K_1K_2	Notes
	1	1400		$K_1 >> K_2$
	1	2.2×10^5		$K_1 >> K_2$
	2		1.1×10^9	$K_2 >> K_1$
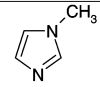	2		1.1×10^{11}	$K_2 >> K_1$
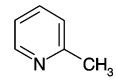	2		~ 3.5×10^5	nonisosbestic $K_2 > K_1$
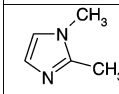	2		~ 2.8×10^8	nonisosbestic $K_2 > K_1$

The formation of the five-coordinate monoquinuclidine adduct of Fe(TATAP) is unexpected, since, as discussed below, treatment of ferrous porphyrins with strong field ligands such as amines usually yields six-coordinate low-spin complexes, such as Fe(TPP)$(piperidine)_2$, which is characterized by X-ray diffraction.[31] These results, however, do not necessarily indicate a fundamental difference in the ligand binding by Fe(TATAP) and Fe(TPP). Quinuclidine, a tertiary amine, may have a larger steric requirement than

(25) (a) Lever, A. *J. Chem. Soc.* **1965**, 1821–1829 and references therein. (b) Dale, B.; Williams, J.; Johnson, C.; Thorp, T. *J. Chem. Phys.* **1968**, *49*, 3441–3444.
(26) Collman, J.; Hoard, J.; Kim, N.; Lang, G.; Reed, C. *J. Am. Chem. Soc.* **1975**, *97*, 2676–2681.
(27) Collman, J. P.; Reed, C. A. *J. Am. Chem. Soc.* **1973**, *95*, 2048–2049.
(28) Collman, J. P.; Gagne, R. R.; Reed, C. A.; Halbert, T. R.; Lang, G.; Robinson, W. T. *J. Am. Chem. Soc.* **1975**, *97*, 1427–1439.
(29) Jaffe, H.; Orchin, M. *Theory and Applications of Ultraviolet Spectroscopy*; Wiley: New York, 1962; pp 578–583.
(30) Brault, D.; Rougee, M. *Biochemistry* **1974**, *13*, 4591–4597.
(31) Radonovich, L. J.; Bloom, A.; Hoard, J. L. *J. Am. Chem. Soc.* **1972**, *94*, 2066–2078.

the secondary amine piperidine. Indeed, the crystal structure referenced above shows unexpectedly long Fe−N_{pip} bonds, which are attributed to close contacts of piperidine hydrogen atoms with the porphyrin core. In addition, as mentioned above for the bis-THF complex, formation of the six-coordinate bis-piperidine complex may be driven by solubility and/or crystal packing forces. We are aware of no solution-phase binding studies of iron(II) porphyrins with quinuclidine.

Spectrophotometric titrations of **4** with unhindered aromatic amines show very different behavior. As shown in Figure 5, new bands appear near 355 and 595 nm, and multiple isosbestic points are maintained throughout the titration. Analysis of the absorbance changes as a function of ligand concentration indicates coordination of two axial bases and, therefore, proves the equilibrium is between the four-coordinate and the six-coordinate complexes (i.e., $K_2 \gg K_1$). The five-coordinate complex, Fe(TATAP)L, is not observed, and only the product of the successive equilibrium binding constants, K_1K_2, can be determined. Similar behavior is observed for ferrous porphyrins[32] and tetraazaporphyrins[8] and has been explained by a decrease in iron spin state from $S = 1$ or 2 to $S = 0$, which causes stronger binding of the second axial ligand compared to that of the first.

The K_1K_2 values reported in Table 3 are similar to those reported in the literature for iron(II) octaethyltetraazaporphyrin but are larger than those reported for iron(II) porphyrins. For example, Brault and Rougee have reported K_1K_2 values of 4×10^7 and 1.3×10^8 for imidazole and pyridine, respectively, binding to deuteroheme in benzene.[30,33]

The different behavior of Fe(TATAP) with aromatic versus nonaromatic nitrogenous bases is surprising; quinuclidine is several orders of magnitude more basic than both 1-methylimidazole and pyridine[34] yet binds only once. This may be a steric effect similar to that observed with 2-substituted imidazoles and ferrous porphyrins.[27] The existence of vacant π^* orbitals on the aromatic amines suggests that iron-to-axial ligand backbonding may also play a role. Electron donation from the iron d_{xz} and d_{yz} orbitals is further consistent with the change in iron spin state on ligand coordination, as discussed above.

Titrations of toluene solutions of **4** with hindered nitrogenous axial ligands (those bearing methyl groups in the 2 position) reveal nonisosbestic changes in the visible spectrum.[35] Nevertheless, at higher concentrations, limiting spectra consistent with the six-coordinate bis-ligated complex, Fe(TATAP)L_2, **6**, are observed. These observations are interpreted as successive binding of two axial ligands where K_2 is only slightly greater than K_1. Steric interactions between the flanking methyl group and the porphyrazine plane result in smaller values of both K_1 and K_2 but a greater reduction in the latter.[26] In the five-coordinate complex, the iron atom can move out of the macrocycle plane toward the axial ligand, thereby reducing repulsions between the methyl group and the macrocycle. However, such relief is not possible in the symmetrical six-coordinate complex. Without the visible spectrum of the pure five-coordinate complex, we were unable to determine individual values of K_1 and K_2, although an estimate was made of their product, K_1K_2 (see Table 3).

Unlike Fe(TATAP), where $K_2 > K_1$, ferrous porphyrins bind two equivalents of hindered nitrogenous ligand with successively smaller binding constants. For example, Basolo reports K_1 and K_2 for the binding of 1,2-dimethylimidazole to iron(II) tetraarylporphyrins as 2.5×10^4 and 2.0, respectively.[36] Because $K_2 << K_1$, the five-coordinate monoligated ferrous porphyrin will predominate in solution at intermediate ligand concentrations. There is no comparable situation in the case of **4** and the hindered aromatic amines. In order to check that our Fe(TATAP) results were not an artifact of low levels of unhindered ligand contaminating our hindered ligand, we titrated Fe(OEP) with our sample of 1,2-Me_2Im and were able to reproduce the five-coordinate complex ($K_1 = 9.7 \times 10^4$), which had a visible spectrum clearly different from that of the six-coordinate complex. It is not apparent why the relative magnitudes of K_2 and K_1 should differ for binding of 2-substituted imidazoles to porphyrins versus tetraazaporphyrins.

Reversible Carbon Monoxide Binding. Fe(TATAP), **4**, reversibly binds carbon monoxide with a noticeable color change from purple to pink. By using the flow method of Collman,[37] various mixtures of CO and N_2 gases, saturated with toluene, were bubbled into a toluene solution of Fe(TATAP) in a cuvette maintained at 25 +/− 0.1 °C. At higher partial pressures of CO, limiting spectra indicative of saturation were observed. The observed changes were completely reversible; one can return to an earlier spectrum by readjusting the gas mixture to a previous CO partial pressure. Changes in the visible spectrum were analyzed as a function of CO partial pressure, as shown in Figure 6.

The presence of multiple isosbestic points indicates a simple equilibrium between **4** and **7**, as shown in Scheme 2. Analysis of the spectra (see Figure 6 inset) shows that only one CO is bound and allows determination of the equilibrium binding constant and $P_{1/2}$(CO), the half-saturation pressure for carbon monoxide. These data are shown in Table 4 along with similar data from the literature.

Comparison of the $P_{1/2}$(CO) values in Table 4 reveals that the two iron porphyrazines, Fe(OETAP) and Fe(TATAP), have comparable CO affinities yet neither is a strong CO binder compared to iron porphyrins: the difference is a factor of 100 or more. The tetraazaporphyrin ligand is considered to be a stronger σ donor and π acceptor than is the porphyrin ligand. This is a result of the smaller metal-binding "hole" and lower energy π MO's in the azaporphyrin. Like

(32) (a) Collman, J. *Acc. Chem. Res.* **1977**, *10*, 265–272. (b) Ellis, P.; Linard, J.; Szymanski, T.; Jones, R.; Dudge, J.; Basolo, F. *J. Am. Chem. Soc.* **1980**, *102*, 1889–1896.

(33) (a) Brault, D.; Rougee, M. *Biochem. Biophys. Res. Commun.* **1974**, *57*, 654–659.

(34) *Handbook of Chemistry and Physics*, 80th ed.; David, R. L., Ed.; CRC Press: New York, 1999.

(35) See Figure 8 in the Supporting Information for changes in the visible spectrum of **4** on titration with 1,2-dimethylimidaole.

(36) Hashimoto, T.; Dyer, R. L.; Crossley, M. J.; Baldwin, J. E.; Basolo, F. *J. Am. Chem. Soc.* **1982**, *104*, 2101–2109.

(37) Collman, J. P.; Brauman, J. I.; Doxsee, K. M.; Halbert, T. R.; Hayes, S. E.; Suslick, K. S. *J. Am. Chem. Soc.* **1978**, *100*, 2761–2766.

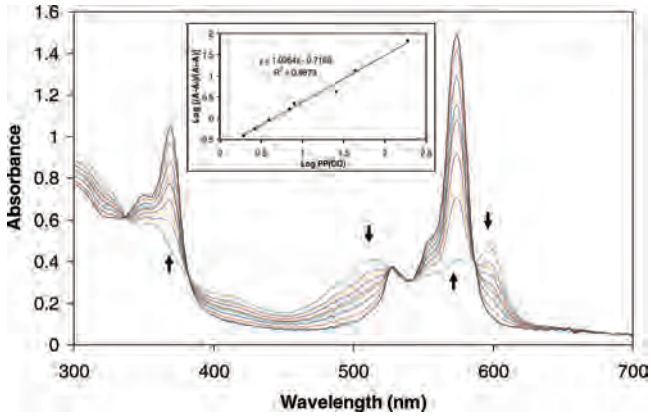

Figure 6. Spectroscopic titration of **4** with CO in toluene containing 1.3 $\times$ 10^{-5} M 1,2-Me_2Im at 25 °C. $[Fe(TATAP)]_{tot}$ = 1.1 $\times$ 10^{-5} M. PPco = 0–760 Torr.

Table 4. $P_{1/2}$(CO) Values for **4** and Related Fe(II) Poprhyrins and Porphyrzines

macrocycle	ligand	[ligand] (M)	$P_{1/2}$(CO) (Torr)	reference/note
OETAP	none		32.1	this work
TATAP	none		17.4	this work
TATAP	1,2-Me_2Im	1.3 $\times$ 10^{-5}	13	this work
TATAP	1-MeIm	1 $\times$ 10^{-6}	4.3	this work
DeutP	1,2-Me_2Im	5 $\times$ 10^{-2}	0.04	*a*, in benzene
OEP	none		0.31	*b*
OEP	1,2-Me_2Im	3 $\times$ 10^{-3}	0. 1	*c*
TPP	none		0.63	*d*, at 20 °C
TPP	1,2-Me_2Im	3.7 $\times$ 10^{-3}	0.14	*e*, at 23 °C
TTPPP	1,2-Me_2Im	2.0 $\times$ 10^{-3}	0.0091	*f*
TpivPP	1,2-Me_2Im	>1.3 $\times$ 10^{-3}	0.0089	*g*
PocPiv	1,2-Me_2Im	0.3	0.067	*c*
C_2-Cap	1,2-Me_2Im	1	0.20	*h*

[a] Rougee, M.; Brault, D. *Biochemistry*, **1975**, *14*, 4100–4106. [b] Strauss, S. H.; Holm, R. H. *Inorg. Chem.* **1982**, *21*, 863–868, at 20 °C. [c] Collman, J. P.; Brauman, J. I.; Iverson, B. L.; Sessler, J. L.; Morris, R. M.; Gibson, Q. H. *J. Am. Chem. Soc.* **1983**, *105*, 3052–3064. [d] Wayland, B. B.; Mehne, L. F.; Swartz, J. *J. Am. Chem. Soc.* **1978**, *100*, 2379–2383. Value of *K*, which was converted to $P_{1/2}$ using the referenced value of Henry's constant for CO in toluene. [e] Hashimoto, T.; Dyer, R. L.; Crossley, M. J.; Baldwin, J. E.; Basolo, F. *J. Am. Chem. Soc.* **1982**, *104*, 2101–2109, at 23 °C. [f] Suslick, K. S.; Fox, M. M.; Reinert, T. J. *J. Am. Chem. Soc.* **1984**, *106*, 4522–4525. [1,2-Me_2Im] calculated based on log K_1 = 4.70 and 99% five-coordinate Fe(TTPPP). [g] Collman, J. P.; Brauman, J. I.; Doxsee, K. M. *Proc. Natl. Acad. Sci. U.S.A.* **1979**, *76*, 6035–6039. [h] Linard, J. E.; Ellsi, P. E., Jr.; Budge, J. R.; Jones, R. D.; Basolo, F. *J. Am. Chem. Soc.* **1980**, *102*, 1896–1904.

tetraazaporphyrin, the carbon monoxide ligand is known to be a strong σ donor and π acceptor. Thus, the lower CO affinity for iron porphyrazines may be due to the lower electron density on the metal available for backbonding to the carbonyl group. Unfortunately, we have not been able to measure the IR stretching frequencies of the iron tetraazaporphyrin carbonyl complexes to further examine this proposal. However, the IR stretching frequencies of the less labile ruthenium(II) carbonyl complexes are known, and these correlate well with the higher π acidity of the porphyrazine ligand compared to that of the porphyrin ligand.[38] Alternatively, the difference in CO affinities could be due to the higher oxidation potential of Fe coordinated by a porphyrazine compared to porphyrin. CO is a strong π acceptor ligand, and any metal that holds onto its electrons more tightly will bind CO less readily. However, the similar CO affinities of Fe(OETAP) and Fe(TATAP) do not correlate with the metal oxidation potential (vide infra).

As can be seen in Table 4, the presence of small amounts of aromatic amines raises the CO affinities of Fe(TATAP), as indicated by slight decreases in the $P_{1/2}$(CO) values. The nitrogenous ligand concentrations were selected based on data in Table 3 such that 90% or more of the Fe(TATAP) remained four-coordinate in the absence of CO. At high nitrogenous ligand concentrations, the CO affinity became negligible due to the lack of an open coordination site. These data are consistent with our earlier observation that Fe(TATAP) binds a second axial ligand more tightly than the first, due to a change in iron spin state. In effect, the nitrogen ligand "primes" the Fe(TATAP) to bind carbon monoxide.

Similar results are seen in the literature where comparable CO binding studies have been done (OEP and TPP), although it should be noted that these are slightly different experiments. In the case of the porphyrins, the concentration of 1,2-Me_2Im is adjusted such that CO is binding to a five-coordinate species. In the case of Fe(TATAP), CO is binding to a four-coordinate iron in the presence of a sixth ligand.

Oxygen Reactivity. Exposure of a toluene solution of **4** to air or pure oxygen (1 atm at room temperature) results in no reaction on the basis of the lack of changes in the visible spectrum. In an effort to enhance its O_2 affinity, Fe(TATAP) was exposed to oxygen in the following: (1) toluene containing 2.0 $\times$ 10^{-5} M 1,2-Me_2Im and (2)*o*-dichlorobenzene, a noncoordinating polar solvent (vide infra). In the former case, no changes were observed in the visible spectrum, and in the latter, Fe(TATAP) extracted Cl from the solvent and formed Fe(TATAP)Cl.

The oxygen reactivity of Fe(TATAP), **4**, is in sharp contrast to the rapid (<5 s), irreversible reaction of unhindered iron(II) porphyrins[39] and tetraazaporphyrins[8,40] with oxygen to give μ-oxo dimers and the rapid but reversible binding of dioxygen by hindered iron(II) porphyrins.[3a] We show above that Fe(TATAP) readily binds nitrogenous ligands and gaseous ligands such as CO. Thus, the lack of O_2 affinity is not due to steric interactions with the flanking anthraceno groups. An alternative interpretation for the above observations is that Fe(TATAP) binds O_2 but the product visible spectrum is identical to that of the reactant. Given the extreme sensitivity of the visible spectrum to changes in metal oxidation and coordination number, this is highly unlikely.

Over the course of several days in air, Fe(TATAP) is oxidized to an unidentified iron(III) product on the basis of changes in the visible spectrum and changes in the magnetic susceptibility in the solid state. Air oxidation of **4** is promoted by the addition of acid; shaking a toluene solution of **4** with 10% aqueous HCl results in rapid formation of chloroiron(III)

(38) ν(CO)'s for Ru(OEP)CO, Ru(OETAP)CO, and Ru(TATAP)CO have been measured at 1976, 2003, and 2027 cm^{-1}, respectively. Similar values have been reported previously for the first two complexes (Whitten et al. *J. Am. Chem. Soc.* **1975**, *97*, 277−281 and Collman et al. *J. Am. Chem. Soc.* **1993**, *115*, 9309−9310).

(39) (a) Chin, D-H.; Del Gaudio, J.; La Mar, G. N.; Balch, A. L. *J. Am. Chem. Soc.* **1977**, *99*, 5486–5488. (b) Chin, D-H.; La Mar, G. N.; Balch, A. L. *J. Am. Chem. Soc.* **1980**, *102*, 4344–4350.

(40) Ercolani, C.; Gardini, M.; Monacelli, F.; Pennesi, G.; Rossi, G. *Inorg. Chem.* **1983**, *22*, 2584–2589.

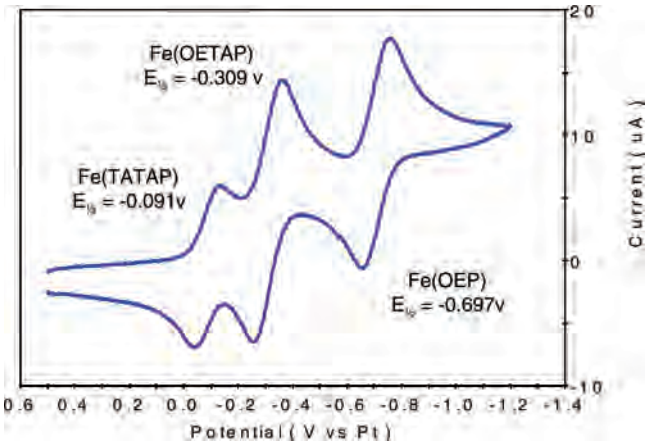

Figure 7. Cyclic voltammetry of Fe(TATAP)(1-MeIm)$_2$ and related complexes.

tetraanthracenotetraazaporphyrin, Fe(TATAP)Cl, **8**. This behavior may indicate the formation of a small amount of Fe(TATAP)-dioxygen adduct, which hydrolyzes to iron(III) and the superoxide ion. Such a mechanism has been proposed for the autoxidation of hemoglobin and myoglobin.[41]

An early discussion of the heme−dioxygen complex included a proposal by Weiss that this complex is best described as an iron(III)−superoxide adduct resulting from electron transfer from the iron to the coordinated dioxygen.[42] Raman studies of the O−O stretching frequencies, including isotopic labeling, support this description, which is now generally accepted.[43] As a result, O_2 affinities of square planar metal complexes of this type are related to the metal oxidation potential[44] and the axial ligand basicity.[45] Since the tetraazaporphyrin ligand is known to shift the III/II oxidation potentials of the bound metal to values higher than those of the analogous porphyrins, lower O_2 affinities are expected for iron(II) tetraazaporphyrins versus those of porphyrins. This is evident in Figure 7.

Figure 7 shows the cyclic voltammogram of a mixture of iron tetraanthracenotetraazaporphyrin, Fe(TATAP), iron octaethyltetraazaporphyrin, Fe(OETAP), and iron octaethylporphyrin, Fe(OEP), in dichloromethane containing an excess of 1-methylimidazole. At the concentration of 1-MeIm used, all three complexes are six-coordinate in both the iron(II) and iron(III) states and show reversible (III/II) couples with a $\Delta i_{peak} \sim 80$ mV in each case. The concentration of each macrocycle was 0.2−0.5 mM; the differences in the current amplitudes in Figure 7 are at least partially due to concentration differences. Cyclic voltammograms of each individual iron complex (not shown) were collected to (1) identify the redox waves in the mixture and (2) check for shifts in redox potentials in the mixture. There were none.

As seen in Figure 7, the two porphyrazines are harder to oxidize than the porphyrin; the Fe(TATAP) redox potential is almost 600 mV positive of that for the Fe(OEP) complex while the Fe(OETAP) derivative is shifted 400 mV positive. Positive shifts in redox couples of metals bound to tetraazaporphyrins compared to porphyrins are expected given the lower energy π MO's of the former. However, we were surprised at the 200 mV difference between the two tetraazaporphyrin complexes. The difference between the two porphyrazines is also apparent in the CO stretching frequencies of the ruthenium carbonyl adducts.[38] We attribute the negligible O_2 affinity of **4** to its positively shifted III/II redox potential. It is difficult to ascribe the different redox properties of these two porphyrazines to the electron donating properties of peripheral ethyl versus anthraceno groups. The 62° dihedral angle and the saturated bridgehead carbon atom between the porphyrazine ring and the flanking benzo groups in Fe(TATAP) preclude electronic coupling between the rings. The oxygen affinity of Fe(OETAP) may also be very low. Its rapid and complete reaction with oxygen may be the result of a multistep process in which highly favored subsequent steps compensate for a low O_2 binding constant.

Suslick notes that the oxygen affinity of ferrous porphyrins correlates with the polarity of the binding "pocket" and the solvent.[46] A more polar local environment stabilizes charge separation in the product iron(III)−superoxide complex. Such an effect may contribute to the low O_2 affinity of Fe(TATAP), which, in toluene, provides a completely nonpolar O_2 binding site. Indeed, the behavior of Suslick's Fe(TTPPP)(1,2-Me$_2$Im) is similar to that of Fe(TATAP), although not as extreme. This five-coordinate iron(II) porphyrin has an unusually low O_2 affinity ($P_{1/2}(O_2) = 508$ Torr in toluene at 25 °C), which is ascribed to the nonpolar O_2 binding site formed by the hydrocarbon superstructure.[17] By comparison, Collman's Fe(TPivPP)(1,2-Me$_2$Im), which has a moderately polar O_2 binding pocket formed by four primary amide "pickets", has a $P_{1/2}(O_2)$ of 38 Torr under identical conditions.[37,47] Suslick further shows an increase in oxygen affinity of Fe(TTPPP)(1,2-Me$_2$Im) as the solvent polarity increases ($P_{1/2}(O_2) = 227$ Torr in *o*-dichlorobenzene at 25 °C) and estimates that binding site polarity can impact $P_{1/2}(O_2)$ values by as much as a factor of 25.

The negligible O_2 affinity of Fe(TATAP) may be partially due to its nonpolar binding site. However, this cannot be the only factor. Even Suslick's Fe(TTPPP)(1,2-Me$_2$Im) complex would be approximately 65% oxygenated at 1 atm partial pressure of oxygen, yet Fe(TATAP) is completely unoxygenated. Assuming Fe(TATAP) is even 5% oxygenated (well within the detection limits of the visible spectroscopy experiment) at 1 atm O_2, one calculates a lower limit of 20 atm (15000 Torr) for the $P_{1/2}(O_2)$ for Fe(TATAP). This represents a minimum 30-fold increase in $P_{1/2}(O_2)$

(41) (a) Shikama, K. *Coord. Chem. Rev.* **1988**, *83*, 73–91. (b) Wallace, W. J.; Houtchens, R. A.; Maxwell, J. C.; Caughey, W. S. *J. Biol. Chem.* **1982**, *257*, 4966–4977. (c) Brantley, R. E., Jr.; Smerdon, S. J.; Wilkinson, A. J.; Singleton, E. W.; Olson, J. S. *J. Biol. Chem.* **1993**, *268*, 6995–7010.
(42) Weiss, J. J. *Nature* **1964**, *202*, 83–84.
(43) Collman, J. P.; Brauman, J. I.; Halbert, T. R.; Suslick, K. S. *Proc. Natl. Acad. Sci. U.S.A.* **1976**, *73*, 3333–3337.
(44) (a) Carter, M. J.; Engelhardt, L. M.; Rillema, D. P.; Basolo, F. *J. Chem. Soc., Chem. Commun.* **1973**, 810–812. (b) Carter, M. J.; Rillema, D. P.; Basolo, F. *J. Am. Chem. Soc.* **1974**, *96*, 392–400. (c) Basolo, F.; Hoffman, B. M.; Ibers, J. A. *Acc. Chem. Res.* **1975**, *8*, 384–392.
(45) Collman, J. P.; Brauman, J. I.; Doxsee, K. M.; Sessler, J. L.; Morris, R. M.; Gibson, Q. H. *Inorg. Chem.* **1983**, *22*, 1427–1432.
(46) Suslick, K. S.; Fox, M. M.; Reinert, T. J. *J. Am. Chem. Soc.* **1984**, *106*, 4522–4525.
(47) Collman, J. P.; Brauman, J. I.; Doxsee, K. M.; Halbert, T. R.; Suslick, K. S. *Proc. Natl. Acad. Sci. U.S.A.* **1978**, *75*, 564–568.

compared to that of Fe(TTPPP) (1,2-Me_2Im) and a minimum 400-fold increase compared to that of Fe(TPivPP)(1,2-Me_2Im). We believe that a positively shifted III/II redox couple is the major factor in the negligible O_2 affinity of Fe(TATAP), **4**.

Conclusions

The synthesis, characterization, structure, and coordination chemistry of iron tetraanthracenotetraazaporphyrin, Fe(TATAP), **4**, and five derivatives are reported. Eight benzo groups flanking the macrocycle periphery form a convex surface on each face of the azaporphyrin and prevent μ-oxo dimer formation. As expected for a 14-electron square planar complex, Fe(TATAP) readily binds a variety of neutral ligands including THF, nitrogenous bases, and carbon monoxide. The equilibrium binding constants for the first two are higher than those of analogous porphyrins while those of the latter are smaller. Fe(TATAP) also shows the different relative magnitudes of successive equilibrium binding constants, K_1 and K_2, for hindered nitrogenous ligands when compared to analogous porphyrins. We attribute these differences to the higher π acidity of the porphyrazine ligand compared to the porphyrin ligand. In contrast to all reported four-coordinate iron(II) porphyrins and azaporphyrins, Fe(TATAP) shows no affinity for O_2. This may be the result of an unusually positive iron(III/II) redox couple and a nonpolar oxygen binding site in Fe(TATAP).

Experimental Section

General Considerations. 11,12-Dicyano-9,10-dihydro-9,10-ethenoanthracene was prepared as described by Smith.[6] All other reagents were purchased commercially and used without further purification except for the toluene and tetrahydrofuran used in the glovebox, which were distilled from sodium/benzophenone ketyl, 1-butanol, which was distilled from magnesium, and nitrogenous ligands, which were distilled from sodium prior to use. Manipulations involving air or water sensitive compounds were done inside a Braun MB150 inert atmosphere glovebox maintained at less than 1 ppm oxygen and water. Samples were submitted to Oneida Research Services Inc., Whitesboro, NY, or to Galbraith Laboratories, Knoxville, TN, for elemental analysis. UV–visible spectra were obtained on a Hewlett-Packard 8452A diode array spectrometer, IR spectra were recorded on either a Perkin-Elmer System 2000 FT-IR or an IR100 spectrometer from Thermo Electron Corporation, ^{1}H NMR spectra were recorded on a JEOL ECX-400 NMR spectrometer (chemical shift values are reported relative to residual protons in the solvent as an internal standard), and mass spectra were recorded on an Applied Biosystems Voyager-DE MALDI-TOF mass spectrometer. Cyclic voltammograms were recorded in dichloromethane containing 0.10 M tetrabutylammonium hexafluorophosphate supporting electrolyte, using a Princeton Applied Research model 173 potentiostat with a model 276 interface. The working electrode was a 1.6 mm platinum disk from Bioanalytical Systems while platinum wire was used as both the reference and working electrodes.

Tetra(9,10-anthraceno)tetraazaporphyrin, H_2(TATAP), 3. A 250 mL round-bottom flask, a magnetic stir bar, a reflux condenser, and a gas inlet tube were dried in an oven prior to use. The cooled round-bottom was charged with 125 mL of dry 1-butanol, and the stir bar, condenser, and gas inlet tube were added. While under an atmosphere of argon, a syringe was used to add 40 mL of 3.0 M methylmagensium iodide in ether solution to the stirred 1-butanol. The addition was made quickly at a rate such that the mixture did not boil over. This mixture was heated to reflux under an argon atmosphere, at which time 15.2 g of solid 11,12-dicyano-9,10-dihydro-9,10-ethenoanthracene, previously ground in a mortar and pestle, was added, and reflux was maintained for 18 h. Within 0.5 h, the solution had turned a dark olive green color, which slowly turned blue over the remaining time. At the end of the heating period, the condenser was set for distillation, and 75 mL of 1-butanol was removed. To the resulting residue was added 50 mL of ethanol, and the mixture was poured into 1 L of a 4/1 water/ethanol mixture, with stirring. The flask was rinsed with small amounts of ethanol. The dark green precipitate was collected by vacuum filtration on a large Büchner funnel, washed with water, and dried under vacuum. The dried precipitate was ground in a mortar and pestle and then extracted into 200 mL of boiling chloroform. This deep blue solution was vacuum-filtered, and the residue was washed with chloroform. The original filtrate and washings were combined and reduced on a rotary evaporator to 100 mL. This chloroform solution was diluted with 100 mL of hexanes, and the resulting mixture was loaded onto a 5 in. long flash silica gel column prepared from the hexanes slurry. Elution of the column with 1/1 hexanes/CH_2Cl_2 removed many colored impurities. Sometimes a royal blue material was eluted. If this was the case, it was collected. Elution with pure dichloromethane gave an intense blue band, which was collected, combined with earlier blue fractions (if any), and reduced to dryness on a rotary evaporator. The resulting blue residue was dissolved in a minimum of chloroform (50 mL); 5 mL of acetic acid was added, and the mixture was heated at reflux for 15 min, after which time the UV–visible spectrum indicated complete demetalation. Cooling this solution followed by filtration gave H_2(TATAP), which was washed with 1/1 hexanes/toluene. Additional product could be obtained from the mother liquor, which was treated, in a separatory funnel, with enough 10% aqueous NaOH solution to neutralize the acetic acid. The organic layer was dried with brine followed by sodium sulfate, filtered, and reduced on a rotary evaporator. Removal of most of the chloroform left microcrystals of H_2(TATAP) suspended in chloroform/toluene/hexanes mother liquor. After drying under vacuum, 1.85 g (12% yield) of the pure macrocycle, identical to that reported by Kopranenkov et al.,[5] was obtained.

Anal. Calcd for $C_{72}H_{42}N_8 \cdot {}^3/_2CHCl_3 \cdot {}^1/_2C_6H_6$: C, 74.26; H, 3.79; N, 9.06. Found: C, 74.09; H, 3.91; N, 8.84. UV–vis (CH_2Cl_2): λ_{max} (nm) (log ε) = 346 (4.82), 412 (4.39), 558 (4.68), 634 (4.85). IR (pure): E_{max} (cm^{-1}) = 3385 (wk), 3097 (wk), 1494, 1122, 985. ^{1}H NMR ($CDCl_3$): δ (ppm) = –3.71 (s, 2H, NH); 7.06 (dd, 16H, J = 5.1, J = 2.9); 7.17 (s, 8H); 7.88 (dd, 16H, J = 5.1, J = 2.9). MS m/z: calcd for M^+ 1018, found 1019.5 (MH^+).

Iron(II) Tetra(9,10-anthraceno)tetraazaporphyrin, Fe(TATAP), 4. Method 1. In an inert atmosphere box, a 500 mL round-bottom flask was charged with 100 mg of anhydrous iron(II) iodide, 100 mg of tetra(9,10-anthraceno)tetraazaporphyrin, 5 drops of 2,6-lutidine, 125 mL of toluene, and 125 mL of THF. This stirred mixture was heated at reflux while the insertion reaction was monitored by removing a small aliquot of the reaction mixture from the glovebox, dissolving it in dichloromethane, and examining the UV–visible spectrum. After 24 h at the reflux temperature, no unmetalated TAP remained. The cooled solution was passed through a small (5 cm length × 2 cm diameter) column of neutral alumina to remove the iron salts. The solvent volume was reduced from the eluent under vacuum in the

glovebox, and hexanes were added to induce crystallization. The crystals were collected by suction, washed with toluene, and dried under vacuum. Yield = 80 mg (80%).

Method 2. A mixture of 50 mg of Fe(TATAP)Cl and 200 mg of zinc powder in 250 mL of a 1/1 toluene/THF solution was stirred at room temperature in an inert atmosphere glovebox for 48 h, after which time, reduction was complete, as indicated by visible spectroscopy. The crude reaction mixture was passed through neutral alumina as described above to remove unreacted zinc metal and zinc salts. The solvent removal under vacuum followed by the addition of hexanes gave microcrystalline Fe(TATAP), which were collected by vacuum filtration, washed with toluene, and dried under vacuum. Yield = 44 mg (88%).

Anal. Calcd for $C_{72}H_{40}N_8Fe \cdot C_7H_8 \cdot THF$: C, 80.57; H, 4.56; N, 9.06. Found: C, 80.75; H, 4.73; N, 9.03. UV–vis (toluene): λ_{max} (nm) (log ε) = 496 (4.42), 554 (4.56), 588 (4.60). IR (pure): E_{max} (cm^{-1}) = 3143 (wk), 1494, 1259, 1131, 1039.

Iron(II) Tetra(9,10-anthraceno)tetraazaporphyrin bispyridine, Fe(TATAP)(pyr)$_2$, 6. Anal. Calcd for $C_{82}H_{52}N_{10}Fe \cdot C_6H_6 \cdot 2H_2O$: C, 79.51; H, 4.55; N, 10.54. Found: C, 79.81; H, 4.33; N, 10.24. UV–vis (toluene): λ_{max} (nm) (log ε) = 356 (4.88), 496 (4.35), 548 (4.50), 570 (4.63), 590 (4.98). IR (pure): E_{max} (cm^{-1}) = 3165 (wk), 1509, 1493, 1259, 1131, 1108, 1038, 754. ^{1}H NMR (C_6D_6 with d_5-pyr): δ (ppm) = 6.89 (dd, 16H, J = 5.0, J = 2.9); 7.24 (s, 8H); 7.59 (dd, 16H, J = 5.0, J = 2.9).

Iron(II) Tetra(9,10-anthraceno)tetraazaporphyrin Carbonyl, Fe(TATAP)CO, 7. UV–vis (toluene): λ_{max} (nm) (log ε) = 368 (4.69), 430 (sh), 530 (sh), 572 (4.93), 654 (3.82).

Iron(III) Tetra(9,10-anthraceno)tetraazaporphyrin Chloride, Fe(TATAP)Cl, 8. Method 1. A mixture of 100 mg of H_2(TATAP) and 100 mg of iron(II) acetate in 50 mL of DMF was heated at the reflux temperature for 12 h, after which time, metalation was complete as indicated by visible spectroscopy. The cooled reaction mixture was poured into water, and the resulting precipitate was collected on Celite. The Celite pad was washed with 200 mL of chloroform, in aliquots, to yield a deep red solution. This was washed twice with 10% aqueous HCl and then passed through a short column of acidic alumina. Several milliliters of toluene were added, and the resulting solution was slowly reduced on a rotary evaporator without heat to give microcrystals of Fe(TATAP)Cl. These were collected by vacuum filtration, washed with toluene, and dried under vacuum. Yield = 81 mg (80%).

Method 2. Crude Fe(TATAP), prepared as described above, was removed from the inert atmosphere glovebox and treated with a few milliliters of dichloromethane. The solution immediately changed color to a deep red. The slow evaporation of the solvent from a chloroform/benzene/THF solution resulted in deposition of crystals, which were collected by vacuum filtration, washed with toluene, and dried under vacuum.

Anal. Calcd for $C_{72}H_{42}N_8FeCl \cdot 2C_6H_6 \cdot THF$: C, 79.07; H, 4.52; N, 8.38. Found: C, 79.25; H, 4.47; N, 8.66. UV–vis (CH_2Cl_2): λ_{max} (nm) (log ε) = 324 (4.66), 432 (4.48), 516 (4.46), 640 (sh), 672 (4.22). IR (pure): E_{max} (cm^{-1}) = 3067 (wk), 1494, 1257, 1129, 1040. MS *m*/*z*: calcd for M^+ 1109, found 1109.2 (M^+), 1073 (MH $-$ Cl^+).

Iron(III) Tetra(9,10-anthraceno)tetraazaporphyrin Hydroxide, Fe(TATAP)OH, 9. Fe(TATAP)Cl, dissolved in dichloromethane, was shaken repeatedly with 1 M aqueous NaOH in a separatory funnel. The red color quickly changed to a deep forest green. The resulting solution was passed through basic alumina, toluene was added to the eluent, and the solvent was slowly reduced in volume on a rotary evaporator to produce a microcrystalline solid. This was collected by vacuum filtration, washed with toluene, dried under vacuum, and stored in an inert atmosphere glovebox.

Anal. Calcd for $C_{72}H_{41}N_8OFe \cdot 2CH_2Cl_2 \cdot C_7H_8$: C, 71.96; H, 3.95; N, 8.29. Found: C, 72.20; H, 4.03; N, 7.85. UV–vis (toluene): λ_{max} (nm) (log ε) = 324 (4.63), 432 (4.45), 506 (4.20), 618 (4.65), 672 (3.86). IR (pure): E_{max} (cm^{-1}) = 3771 (wk), 3056 (wk), 1505, 1494, 1257, 1129, 1033. MS *m*/*z*: calcd for M^+ 1089, found 1088.9 (M^+), 1073 (MH $-$ OH^+).

X-ray Crystallography of 8. The slow evaporation of the solvent from a benzene/chloroform solution caused large, cubic crystals of **8** to be deposited. A crystal suitable for crystallographic structure determination was selected, mounted on a glass fiber held in a copper mounting-pin, and transferred to the 123 K N_2 cold stream of a Siemens SMART CCD diffractometer equipped with a Siemens LT-3 low-temperature device. A preliminary unit cell determination was accomplished using reflections harvested from three orthogonal sets of twenty frames (0.3° ω scans). The final unit cell parameters were refined using reflections with $I > 10\sigma(I)$, harvested from the entire data collection. All data were corrected for Lorentz and polarization effects, as well as for absorption. Structure solution by direct methods in space group $P\bar{1}$ revealed the non-hydrogen atoms of the Fe(TATAP) moiety. Subsequent difference maps following cycles of least-squares refinement indicated unresolved residual density that could not be modeled into sensible solvent molecules. Using the SQUEEZE routine of PLATON, void space and residual density were found that were consistent with two molecules of benzene and six of chloroform per unit cell. Details of the structure determination are given in the cif file, available as Supporting Information.

Supporting Information Available: Visible spectrum changes (nonisosbestic) for **4** when titrated with a hindered nitrogenous ligand, 1,2-dimethylimidazole. X-ray crystallographic results for **8** in CIF format. This material is available free of charge via the Internet at http://pubs.acs.org.

IC702149Z